Small-scale magnetic fields on late-type M-dwarfs

S.B.F. DORCH[1,2] and H.-G. LUDWIG[3]

[1] The Niels Bohr Institute for Astronomy, Physics and Geophysics, Juliane Maries Vej 30, DK-2100 Copenhagen Ø, Denmark
[2] The Institute for Solar Physics of the Royal Swedish Academy of Sciences, SCFAB, SE-10691 Stockholm, Sweden
[3] Lund Observatory, Box 43, S-22100 Lund, Sweden

Received 2002 May 3; accepted 2002 July 3

Abstract. We performed kinematic studies of the evolution of small-scale magnetic fields in the surface layers of M-dwarfs. We solved the induction equation for a prescribed velocity field, magnetic Reynolds number $\mathrm{Re_M}$, and boundary conditions in a Cartesian box, representing a volume comprising the optically thin stellar atmosphere and the uppermost part of the optically thick convective envelope. The velocity field is spatially and temporally variable, and stems from detailed radiation-hydrodynamics simulations of convective flows in a proto-typical late-type M-dwarf ($T_{\rm eff} = 2800\,\mathrm{K}, \log g = 5.0$, solar chemical composition, spectral type ≈M6). We find dynamo action for $\mathrm{Re_M} \geq 400$. Growth time scales of the magnetic field are comparable to the convective turn-over time scale (≈ 150 sec). The convective velocity field concentrates the magnetic field in sheets and tubular structures in the inter-granular downflows. Scaling from solar conditions suggests that field strengths as high as 20 kG might be reached locally. Perhaps surprisingly, $\mathrm{Re_M}$ is of order unity in the surface layers of cooler M-dwarfs, rendering the dynamo inoperative. In all studied cases we find a rather low spatial filling factor of the magnetic field.

Key words: stars: activity – stars: low-mass – stars: magnetic fields

1. Introduction

M-type dwarfs show the highest degree of magnetic activity. Besides X-ray and H_α emission as indirect tracers, Zeeman broadening of magnetically sensitive photospheric lines has been observed (Johns-Krull & Valenti 1996, Kochukhov et al. 2001). The photospheric lines show no rotational modulation or net polarization, indicating that fields of *small scale* (relative to the star's radius) exist on the surfaces of M-dwarfs. These fields can have an appreciable strength (few kG), and can cover a substantial area (filling factors up to 50 %).

Little is known about the structure of magnetic fields in the photospheres of M-dwarfs. From an observational point of view one would like to get some input from theory, that would alleviate the problem of disentangling field strength and filling factor. To this end we started to investigate the kinematic effect of the convective velocity field on a magnetic seed field. This has become possible due to recent progress in the hydrodynamical modeling of atmospheres in the regime of cool M-dwarfs (Ludwig, Allard, & Hauschildt 2002). The present investigation is targeting at an application to spectroscopy, meaning that we focus on layers near optical depth unity. To overcome partially the limits stemming from the restriction to the kinematic magneto-hydrodynamics regime (hereafter "kinematic MHD"), we tried to relate our results to the situation in the Sun, emphasizing the scaling from familiar solar conditions to M-dwarfs.

Correspondence to: dorch@astro.ku.dk

2. Model setup

2.1. The convective velocity

The velocity field was taken from a radiation-hydrodynamics simulation of a prototypical M-dwarf atmosphere (Ludwig et a. 2002, see Fig 1) of $T_{\rm eff} = 2800\,\mathrm{K}$, $\log g = 5.0$, and solar chemical composition (corresponding to a spectral type of ≈M6). The 3D radiation-hydrodynamics code of Nordlund & Stein (Stein & Nordlund 1998, and references therein) has been adapted for this purpose. The code treats the interaction of radiation and gas flows in detail, rotation and magnetic fields are neglected. Rotation has only a minor effect on the structure of the convective flows near the stellar surface due to the short convective turn-over time scales (relative to typical rotation periods of several hours or longer). Magnetic fields can potentially influence the flow structure significantly

 0004-6337/02/3-408-0402 $ 17.50+.50/0

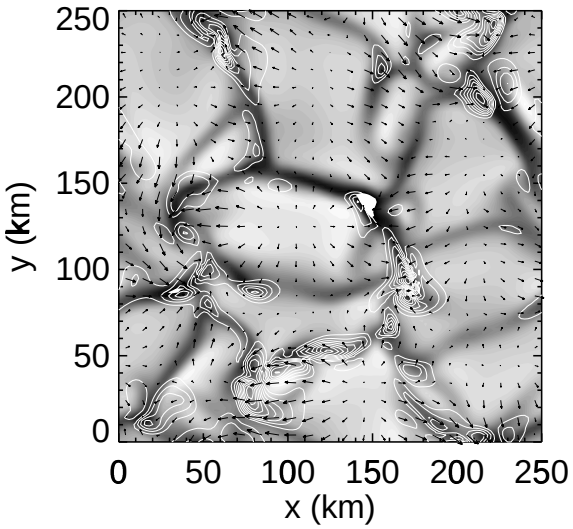

Fig. 1. Snapshot of the vertical component of the magnetic field at optical depth unity (**contours**), emergent intensity (**grey tones**), and the velocity field (**arrows**) towards the end of an evolutionary sequence of an unquenched model with $\mathrm{Re_M}$=20.

provided the field is strong, i.e. dynamically important. However, this corresponds to the full MHD case which is beyond the scope of this paper. We selected a temporal sequence towards the end of the simulation run, which comprises 1500 s of stellar time, corresponding to roughly 10 convective turnover time scales. The sequence consists of 150 snapshots of the flow field, each comprising $125 \times 125 \times 82$ grid points corresponding to $250 \times 250 \times 87\,\mathrm{km}^3$ in geometrical size. At any instant in time about 10 granular cells were present in the computational domain, ensuring a statistically representative ensemble. M-dwarf granulation is on the qualitative level similar to the solar granulation. Quantitatively, there are differences which are discussed below where relevant.

2.2. Kinematic magneto-hydrodynamics

We assume the kinematic regime of MHD, where one neglects the back-reaction of the magnetic field on the fluid motions. This means that the non-linear behavior cannot be rendered correctly in this regime, which is also sometimes referred to as the linear regime of MHD. Then solving the MHD equations reduces to the problem of seeking the solution to the time-dependent induction equation:

$$\frac{\partial \mathbf{B}}{\partial t} = \nabla \times (\mathbf{u} \times \mathbf{B}) + \eta \nabla^2 \mathbf{B}, \qquad (1)$$

where $\mathbf{u}$ is the prescribed velocity field (from the radiation-hydrodynamic simulation), $\mathbf{B}$ the magnetic field, and η the magnetic diffusivity. We assume a spatially constant magnetic diffusivity. Note, that the problem is linear on this level of approximation. We vary the magnetic diffusion by setting the magnetic Reynolds number $\mathrm{Re_M}$ which is defined as $\mathrm{Re_M} = \mathrm{U}\ell/\eta$, where U is a characteristic velocity, ℓ a characteristic length scale, and η the magnetic diffusivity, which in turn is related to the electrical conductivity σ through $\eta = 1/\mu\sigma$.

We solve Eq. (1) using staggered variables on the grid of the hydrodynamical flow field. The numerical method was originally developed by Galsgaard and others (Galsgaard & Nordlund 1997) for general MHD purposes. A special version is the code used by Archontis & Dorch (Dorch 2000; Archontis, Dorch, & Nordlund 2002) to study dynamo action in prescribed flows.

We kept the same velocity field, and studied different magnetic diffusivities. To first order we hope to represent the different conditions encountered in various M-dwarf atmospheres by the the change of magnetic diffusivities.

2.3. Magnetic quenching of the velocity field

The kinematic approximation to the MHD equations — i.e. neglecting the back-reaction of the magnetic field by omitting the Lorentz force in the equation of motion — becomes inaccurate when the magnetic field becomes sufficiently strong. That is, when the magnetic energy density approaches equipartition with the kinetic energy density, corresponding to a field strength $\mathrm{B_{eq}} = \mathrm{u}\sqrt{\mu\rho}$. One can try to capture the effect of a near-equipartition magnetic field, by utilizing a quenched velocity field that has a reduced amplitude in the regions where the magnetic field is strong. In a few cases we employed such a quenched velocity field when solving the induction equation Eq. (1). The quenched velocity field $\mathbf{u}_\mathrm{q}$ was modeled according to

$$\mathbf{u}_\mathrm{q} = \mathbf{u}\ \exp -\alpha(e_\mathrm{M}/e_\mathrm{K})^2, \qquad (2)$$

where α is a constant, e_M the local magnetic energy density, e_K the average kinetic energy density, taken to be constant in time and space. The quenching reduces the velocity amplitude at locations where the magnetic energy (or field) becomes comparable to the kinetic energy of the fluid motions: it thus reduces the growth of the magnetic field in these regions causing it to saturate. We chose $\alpha = 1.75$ which ensures $\mathbf{u}_\mathrm{q} \approx \mathbf{u}$ up to field strength of 10% of $\mathrm{B_{eq}}$, and $\mathbf{u}_\mathrm{q} \approx 0$ at a field strength of 1.2 times equipartition. Note, that this quenching procedure makes the problem non-linear in B, and that a constant e_K merely introduces a scaling factor in the solution, i.e. its concrete value is unimportant. In future work we plan to replace Eq. (2) with a more realistic quenching expression, taking into account the geometry of the flow and the magnetic field.

2.4. Initial and boundary conditions

The numerical method used to solve Eq. (1) by default considers periodic boundary conditions in all three dimensions. We implement non-periodic vertical boundary conditions through "ghost zones" at the top and bottom of the domain: then one may constrain the magnetic field to be vertical (horizontal) by requiring its horizontal (vertical) component(s) to be anti-symmetric across the boundary, and the remaining component(s) to be symmetric.

The initial magnetic field is either uni-directional (vertical or horizontal) or smoothly varying on small scales. The initial field strength $\mathrm{B_0}$ is set to be much smaller than $\mathrm{B_{eq}}$ (only relevant for the cases with quenched velocity field).

3. Results

3.1. Magnetic Reynolds numbers of order unity in cooler M-dwarfs

In the following we discuss kinematic MHD models with $\mathrm{Re_M}$ as low as 20. In the astrophysical context, low values of $\mathrm{Re_M}$ are uncommon, mostly due to the large spatial scales usually involved. However, in M-dwarf atmospheres we can be confronted with the situation of rather low $\mathrm{Re_M}$ (Meyer & Meyer-Hofmeister 1999): Fig. 2 shows the ratio of electron to gas pressure, and $\mathrm{Re_M}$ in the $T_{\rm eff} = 2800\,\mathrm{K}$ M-dwarf model as well as the Sun. $\mathrm{Re_M}$ has been evaluated assuming constant typical length and velocity scales independent of depth[1]. $\mathrm{Re_M}$ primarily reflects the run of the electric conductivity in the atmosphere, which in turn is mostly controlled by the electron to gas pressure. The conductivity has been evaluated assuming a weakly ionized plasma (Kopecký 1957, as quoted by Stix 1989).

Even if one concedes an appreciable degree of uncertainty related to the choice of scales, at sufficiently cool temperatures $\mathrm{Re_M}$ reaches order unity in the surface layers. This is a consequence of the declining electron density, the shrinking of spatial scales (due to smaller pressure scale heights), and smaller convective velocities (due to lower energy fluxes and higher atmospheric densities). This refers to the surface layers. Qualitatively, we expect a strong increase of $\mathrm{Re_M}$ with depth, and beyond a certain depth the regime of $\mathrm{Re_M} > 1$ is reached again. However, gas motions in this depth will generally be slower and the tangling of magnetic field lines less rapid, which may reduce the efficiency of chromospheric and coronal heating. Whether this plays a role for the observed decline of stellar activity at the transition from M- to L-dwarfs (Gizis et al. 2000) is presently a matter of debate (Mohanty et al. 2002, Berger 2002).

3.2. Scaling of the field strength

In order to obtain an estimate of the field strength to be expected in M-dwarf atmospheres — provided local conditions indeed control its value — we compared kinetic energy densities and pressures obtained from our M-dwarf radiation-hydrodynamics model with a similar model computed for the Sun. Figure 3 shows that the kinetic energy densities in the surface layer of our reference M-dwarf model are systematically smaller than in the Sun, but only within a factor of 2. At the $\tau = 1$ level the pressure is higher by a factor of 12 and density by a factor of 42 in the M-dwarf model relative to a solar model (not shown). Assuming a scaling of the magnetic field with gas pressure, we expect a maximum field strength in flux concentrations of about 10 times the solar value, or about 20 kG if one scales values found in magneto-hydrodynamical simulations for the Sun (Stein et al. 1999). However, the kinetic energy densities point towards a field of slightly sub-solar field strengths.

[1] Sun: $\ell = 1500\,\mathrm{km}$, $v = 2.4\,\mathrm{km/s}$; Mdwarf: $\ell = 80\,\mathrm{km}$, $v = 0.16\,\mathrm{km/s}$

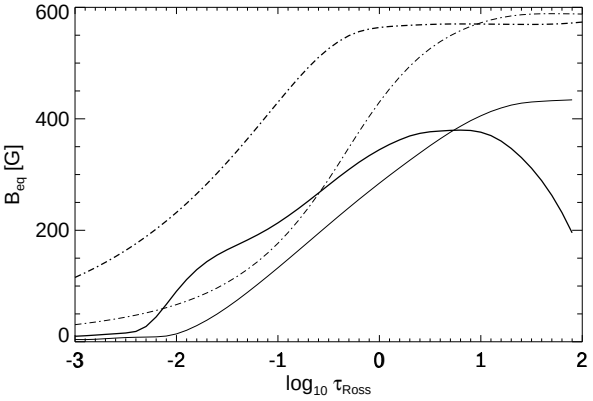

Fig. 3. Kinetic energy densities expressed in terms of the corresponding equipartition field strength as a function of Rosseland optical depth. Depicted are results from hydrodynamical simulations for the $T_{\rm eff} = 2800\,\mathrm{K}$ M-dwarf (**solid lines**) and the Sun (**dash-dotted lines**). The total kinetic energy density is broken into contribution of horizontal (**thick lines**) and vertical motions (**thin lines**).

3.3. Dynamo action and magnetic Reynolds number

A flow is a fast (kinematic) dynamo when the exponential growth rate γ is positive, where

$$\gamma = \lim_{\eta\to 0} \gamma_\eta = \lim_{\eta\to 0} \lim_{t\to\infty} \log(\mathrm{E_M}(t)/\mathrm{E_M}(0))/t, \qquad (3)$$

where $\mathrm{E_M}$ is the total magnetic energy, and γ_η is the growth rate at a specific diffusivity, corresponding to a certain $\mathrm{Re_M}$. That is, fast dynamo action requires a continuous increase of magnetic energy, even in the limit of vanishing diffusivity. This limit is relevant because most astrophysical systems have $\mathrm{Re_M} \gg 1$ and small but non-zero η. It is believed (but not proven) that turbulent astrophysical systems are fast dynamos operating at $\mathrm{Re_M} \gg 1$. When $\mathrm{Re_M}$ increases, the length scale of magnetic islands decreases and scales as $\mathrm{Re_M^{-\frac{1}{2}}}$. There is a maximum value of $\mathrm{Re_M}$, which can be achieved with our numerical resolution $\Delta x = 2$ km, and therefore the largest magnetic Reynolds number that we can allow is of the order of 400 corresponding to 2 Δx (the Nyquist wavelength). Figure 4 shows the two-dimensional power spectrum of the total magnetic field and its vertical component at optical depth unity in the case $\mathrm{Re_M} = 100$: the power on small-scales close to the resolution limit is much less than on the granulation scale. Hence in the following, we concentrate on situations with $\mathrm{Re_M} \leq 400$.

3.4. Kinematic models

In the absence of non-linear effects, in case of a dynamo, one expects a continuing exponential growth of $\mathrm{E_M}$. Figure 5 shows the result in terms of $\mathrm{E_M}(t)$ for five different models corresponding to varying $\mathrm{Re_M}$: most of the models in fact are dominated by decaying modes, with negative growth rates $\gamma_\eta < 0$. In particular, the case with $\mathrm{Re_M}$= 20 (high diffusion) is clearly an example of an anti-dynamo: the diffusion works faster than the flows can sweep up the field and concentrate it in the inter-granular downdraft lanes, and the dominant magnetic mode is a decaying one. Increasing $\mathrm{Re_M}$ decreases γ_η

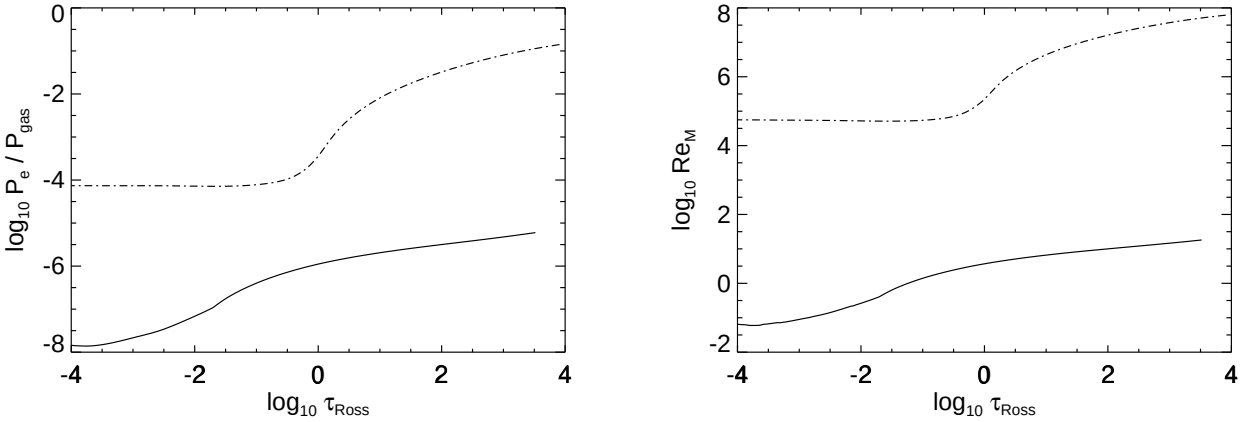

Fig. 2. The ratio of electron to gas pressure (**left panel**), and the magnetic Reynolds number (**right panel**) as a function of Rosseland optical depth in a $T_{\rm eff} = 2800$ K M-dwarf (**solid line**) and a solar model atmosphere (**dashed line**). Note the low magnetic Reynolds number in the M-dwarf model, primarily reflecting the low electric conductivity of the stellar gas in the rather cool M-dwarf atmosphere.

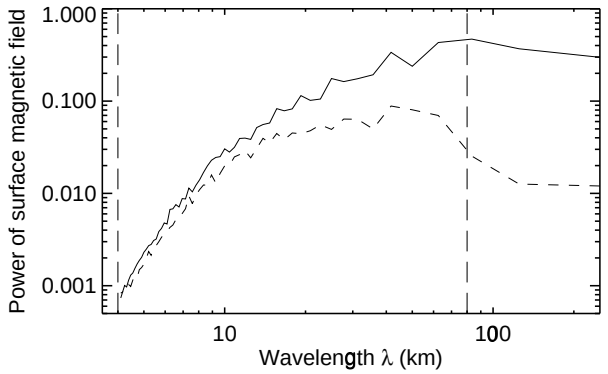

Fig. 4. The power of the magnetic field at the surface ($\tau = 1$) in a model with $\mathrm{Re_M} = 100$. Shown are the total field strength (**full curve**) and the vertical field component (**dashed**). The vertical lines indicate the Nyquist wavelength (**left**) and the typical size of the granular cells (**right**).

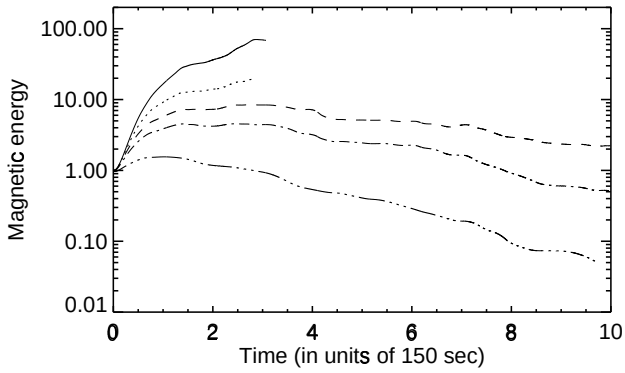

Fig. 5. The total magnetic energy $\mathrm{E_M}/\mathrm{E_0}$ as a function of time in units of 150 seconds (the typical convective turn-over time). Five models are presented, with different amounts of diffusion: $\mathrm{Re_M} =$ 800 (**full**), 400 (**dotted**), 200 (**dashed**), 100 (**dashed dotted**), and 20 (**dashed triple dotted curve**).

(numerically), so that for $\mathrm{Re_M} = 200$ the decay time is 40 time longer than at $\mathrm{Re_M} = 20$. In terms of providing dynamo action, the most promising cases are those with lower diffusion and $\mathrm{Re_M} > 300$–400: at $\mathrm{Re_M} = 400$ a growing mode seems to be dominating. One of the models in Fig. 5 had $\mathrm{Re_M} = 800$, i.e. it produced magnetic structures too small to be resolved, and therefore magnetic energy is lost from the computational domain and $\mathrm{E_M}$ seems to saturate because of enhanced numerical diffusion.

In the high diffusion case (e.g. $\mathrm{Re_M} = 20$) the magnetic field varies smoothly across the domain, and its power peaks on scales approximately $\ell \approx 50$ km when considering B_z (see Fig 1). At higher $\mathrm{Re_M}$ more small scales are generated mostly around the downdraft lanes.

3.5. Quenched models

To examine the structure of the magnetic field in the high $\mathrm{Re_M}$ cases with dynamo action, we computed a few models including the quenching mentioned above: quenching the velocity field only affects those models that are dominated by growing modes ($\gamma_\eta > 0$). In case of a low $\mathrm{Re_M}$, the results remain unchanged since the field never becomes comparable to $\mathrm{B_{eq}}$. For $\mathrm{Re_M} = 200$ the dominant mode is still decaying. At $\mathrm{Re_M} = 400$ the field is amplified until it approaches equipartition and the quenching causes $\mathrm{E_M}$ to saturate; see Fig. 6. At the time of saturation there is a lot of power at small scales close to the resolution limit, but the main power is concentrated at larger scales around 100 km. The saturation level is artificially fixed by our choice of quenching function Eq. (2), the value of α, and our choice of a constant value of $e_{\rm K}$. Hence our simulation results in no direct information on the amplitude of the magnetic field, only on the geometry that one may expect in a non-linear simulation.

Figure 7 shows the PDFs of B_z for three different values of $\mathrm{Re_M}$: the broad distribution of field strengths for low $\mathrm{Re_M}$ should be seen in contrast to the narrow one for high $\mathrm{Re_M}$. At any time the strongest part of the field occupies only a very small part of the volume no matter what the level of

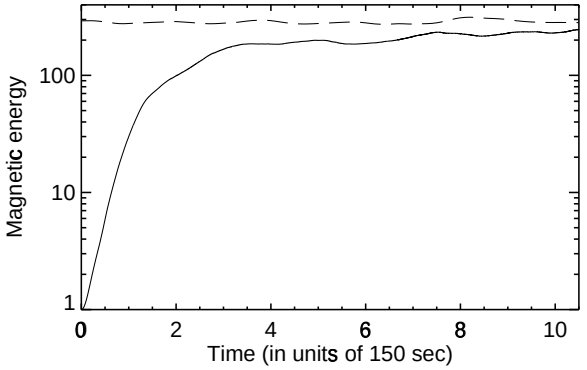

Fig. 6. The total magnetic energy $\mathrm{E_M}/\mathrm{E_0}$ as a function of time for a model with $\mathrm{Re_M}$= 400 and a quenched velocity field (**full**). Also shown is the total available kinetic energy (**dashed curve**).

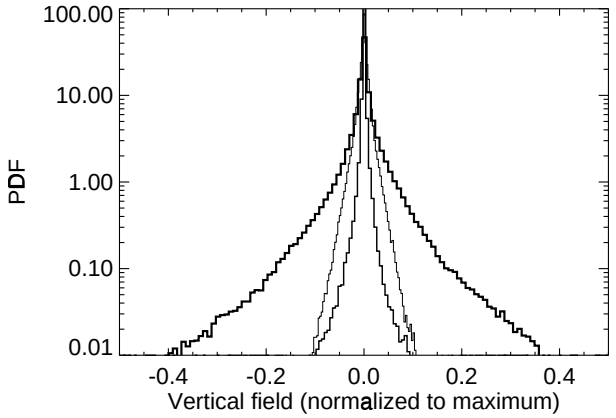

Fig. 7. The probability distribution function (PDF) of the vertical field component around optical depth unity. Lines show the distribution in unquenched models for magnetic Reynolds numbers $\mathrm{Re_M} = 20, 400, 200$ "outside-in" of the hat shaped PDFs. Note the non-monotonic behaviour with $\mathrm{Re_M}$.

diffusion is, but for low $\mathrm{Re_M}$ the preference for strong fields is less pronounced; the field is less intermittent. We attribute the non-monotonic behavior of the models displayed in Fig. 7 to the model with $\mathrm{Re_M} = 400$ showing dynamo action while the others do not.

4. Conclusions

- The geometry of small-scale (i.e. locally generated or modulated) magnetic fields looks similar to the situation for the Sun (i.e. mostly located in the intergranular lanes). The basic reason is that M-dwarf granulation is qualitatively similar to solar granulation.
- There are differences due to potentially quite different magnetic diffusivities (and values of $\mathrm{Re_M}$).
- Depending on $\mathrm{Re_M}$ we get or do not get local dynamo action.
- Since we are making a kinematic study, the absolute field strength is undefined. Scaling from the Sun would suggest flux tubes with up to factor 10 higher fields (assuming equipartition with the gas pressure), or slightly sub-solar (within a factor 2) fields (assuming equipartition with the kinetic energy density).

Acknowledgements. SBFD was supported through an EC-TMR grant to the European Solar Magnetometry Network. HGL acknowledges financial support of the Walter Gyllenberg Foundation, and the Swedish Vetenskapsrådet.

References

Archontis, V.D., Dorch, S.B.F., Nordlund, Å.: 2002, submitted to A&A (preprint astro-ph/0204208)
Berger, E.: 2002, preprint astro-ph/0111317
Dorch, S.B.F.: 2000, PhyS 61, 717
Galsgaard, K., Nordlund, Å.: 1997, JGR 102, 219
Gizis, J.E., Monet, D.G., Reid, N.I., Kirkpatrick, J.D., Libert, J., Williams, R.J.: 2000, AJ 120, 1085
Johns-Krull, C.M., Valenti, J.A.:1996, AJ 459, L95
Kochukhov, O.P., Piskunov, N.E., Valenti, J.A., Johns-Krull, C.M.: 2001, in: R.J. García López, R. Rebolo, M.R. Zapatero Osorio (eds.), *The 11^{th} Workshop on Cool Stars, Stellar Systems and the Sun*, ASP Conf. Ser. 223, 985
Kopecký, M.: 1957, Bull. Astron. Inst. Czech. 8, 71
Ludwig, H.-G., Allard, F., Hauschildt, P.H.: 2002, submitted to A&A
Meyer, F., Meyer-Hofmeister, E.: 1999, A&A 341, L23
Mohanty, S., Basri, G., Shu, F., Allard, F., Chabrier, G.: 2002, ApJ 571, 469
Stein, R.F., Nordlund, Å.: 1998, ApJ 499, 914
Stein, R.F., Georgobiani, D., Bercik, D.J., Brandenburg, A., Nordlund, Å.: 1999, in: Á. Giménez, E.F. Guinan, B. Montesinos (eds.), *Theory and Tests of Convection in Stellar Structure*, ASP Conf. Ser. 173, 193
Stix, M.: 1989, *The Sun: An Introduction*, Springer